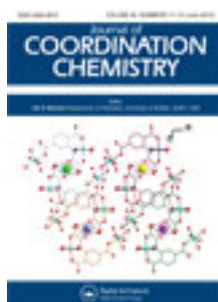


This article was downloaded by: [Renmin University of China]

On: 13 October 2013, At: 10:34

Publisher: Taylor & Francis

Informa Ltd Registered in England and Wales Registered Number: 1072954 Registered office: Mortimer House, 37-41 Mortimer Street, London W1T 3JH, UK



Journal of Coordination Chemistry

Publication details, including instructions for authors and subscription information:

<http://www.tandfonline.com/loi/gcoo20>

DNA-binding and cleavage activity of polypyridyl ruthenium(II) complexes

Mohan N. Patel^a, Deepen S. Gandhi^a, Pradhuman A. Parmar^a & Hardik N. Joshi^a

^a Department of Chemistry, Sardar Patel University, Vallabh Vidyanagar-388 120, Gujarat, India

Published online: 10 May 2012.

To cite this article: Mohan N. Patel, Deepen S. Gandhi, Pradhuman A. Parmar & Hardik N. Joshi (2012) DNA-binding and cleavage activity of polypyridyl ruthenium(II) complexes, Journal of Coordination Chemistry, 65:11, 1926-1936, DOI: [10.1080/00958972.2012.685728](https://doi.org/10.1080/00958972.2012.685728)

To link to this article: <http://dx.doi.org/10.1080/00958972.2012.685728>

PLEASE SCROLL DOWN FOR ARTICLE

Taylor & Francis makes every effort to ensure the accuracy of all the information (the "Content") contained in the publications on our platform. However, Taylor & Francis, our agents, and our licensors make no representations or warranties whatsoever as to the accuracy, completeness, or suitability for any purpose of the Content. Any opinions and views expressed in this publication are the opinions and views of the authors, and are not the views of or endorsed by Taylor & Francis. The accuracy of the Content should not be relied upon and should be independently verified with primary sources of information. Taylor and Francis shall not be liable for any losses, actions, claims, proceedings, demands, costs, expenses, damages, and other liabilities whatsoever or howsoever caused arising directly or indirectly in connection with, in relation to or arising out of the use of the Content.

This article may be used for research, teaching, and private study purposes. Any substantial or systematic reproduction, redistribution, reselling, loan, sub-licensing, systematic supply, or distribution in any form to anyone is expressly forbidden. Terms & Conditions of access and use can be found at <http://www.tandfonline.com/page/terms-and-conditions>

DNA-binding and cleavage activity of polypyridyl ruthenium(II) complexes

MOHAN N. PATEL*, DEEPEN S. GANDHI, PRADHUMAN A. PARMAR
and HARDIK N. JOSHI

Department of Chemistry, Sardar Patel University, Vallabh
Vidyanagar–388 120, Gujarat, India

(Received 26 September 2011; in final form 8 March 2012)

Polypyridyl ruthenium(II) complexes $[\text{Ru}^{\text{II}}(3\text{-bptpy})(\text{dmphen})\text{Cl}]\text{ClO}_4$ (1), $[\text{Ru}^{\text{II}}(3\text{-cptpy})(\text{dmphen})\text{Cl}]\text{ClO}_4$ (2), $[\text{Ru}^{\text{II}}(2\text{-tptpy})(\text{dmphen})\text{Cl}]\text{ClO}_4$ (3), and $[\text{Ru}^{\text{II}}(9\text{-atpy})(\text{dmphen})\text{Cl}]\text{ClO}_4$ (4) {where 3-bptpy = 4'-(3-bromophenyl)-2,2':6',2''-terpyridine, 3-cptpy = 4'-(3-chlorophenyl)-2,2':6',2''-terpyridine, 2-tptpy = 4'-(2-thiophenyl)-2,2':6',2''-terpyridine, 9-atpy = 4'-(9-anthryl)-2,2':6',2''-terpyridine, dmphen = 2,9-dimethyl-1,10-phenanthroline} have been synthesized and characterized. The DNA-binding properties of the complexes with Herring Sperm DNA have been investigated by absorption titration and viscosity measurements. The ability of complexes to break the pUC19 DNA has been checked by gel electrophoresis. The experimental results suggest that all the complexes bind DNA *via* partial intercalation. The results also show that the order of DNA-binding affinities of the complexes is $4 < 3 < 2 < 1$, confirming that planarity of the ligand in a complex is very important for DNA-binding.

Keywords: Terpyridine; Ruthenium(II) complexes; pUC19; DNA-binding and cleavage

1. Introduction

Ru^{II} complexes have been investigated as potent agent in chemotherapy and photodynamic therapy for their high affinity to double-strand DNA helix [1]. DNA-binding mechanism and behavior of the complexes are closely related to size, shape, and planarity of the intercalative ligands. Ancillary ligands also play an important role in DNA-binding of complexes [2]. Polypyridyl complexes of ruthenium are intensely colored due to localized metal-to-ligand charge transfer (MLCT) transition. This MLCT transition is particularly important as it is perturbed when the complex interacts with DNA, providing a spectroscopic probe. Polypyridyl Ru^{II} complexes can bind to DNA *via* non-covalent interactions such as electrostatic, groove and intercalative binding, which includes classical intercalation, semi-intercalation, and quasi-intercalation [3].

In 1931, terpyridines were isolated by Morgan and Burstall [4] when they heated pyridine and dry FeCl_3 to 340°C in an autoclave (50 atm) for 36 h. Afterwards, addition of Fe(II) to the solution gave purple color denoting formation of metal complex.

*Corresponding author. Email: jeenen@gmail.com

Considerable research has been dedicated to better understand and utilize terpyridine metal complexes with a wide variety of transition metals and lanthanides, in order to use their unique photophysical, electrochemical, magnetic, optical properties, and biological activities. Due to these characteristics, terpyridine metal complexes have potential applications, such as dye-sensitized solar cells [5], photosensitizers [6], photocatalysis [7], luminescent chemosensors [8], light-emitting diodes [9], homogeneous assays [10], DNA-binding [11], antigens [12], anti-tumor [13] and anti-microbial agents [14], and magnetic resonance imaging contrast agents [15]. Self-assembly of terpyridine metal complexes on different surfaces [16] have promising roles in nanomolecular devices [17].

Ruthenium(II) polypyridine complexes display unique photophysical and redox properties [18, 19]. To generate ruthenium complexes as DNA probes and potential chemotherapeutic agents, a large number of ruthenium complexes containing tpy as an auxiliary ligand have been synthesized and their DNA-binding and cleavage activity have been examined [20, 21]. Most of the reported complexes contain only bidentate or tridentate ligands, while here bidentate (2,9-dimethyl-1,10-phenanthroline) and tridentate (substituted terpyridines) ligands have been used to synthesize mononuclear complexes. We mainly focus on metal complex interaction with DNA.

In continuation of our previous work [22], we report synthesis and characterization of polypyridyl complexes of ruthenium using terpyridines and 2,9-dimethyl-1,10-phenanthroline (dmphen). Absorption titration and viscosity measurement have been used to study the interaction of these complexes with DNA; cleavage ability of the complexes has been checked using gel electrophoresis.

2. Experimental

2.1. Materials

2-Acetyl pyridine, 3-chlorobenzaldehyde, 3-bromobenzaldehyde, thiophene-2-carbaldehyde, and 9-anthraldehyde were purchased from Spectrochem (Mumbai, India). Ruthenium trichloride and sodium perchlorate were purchased from Chemport (Mumbai, India). Agarose, ethidium bromide (EB), Tris-Acetate-EDTA (TAE), bromophenol blue, and xylene cyanol FF were purchased from Himedia (India). Herring Sperm DNA was purchased from Sigma Chemical Co. (India). 2,9-Dimethyl-1,10-phenanthroline was purchased from Loba chemie (India). Culture of pUC19 bacteria (MTCC 47) was purchased from the Institute of Microbial Technology (Chandigarh, India).

2.2. Physical measurements

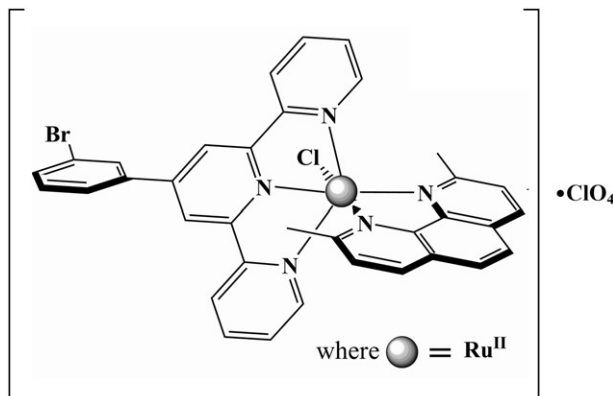
Infrared (IR) spectra were recorded on a Fourier transform IR (FTIR) Shimadzu spectrophotometer as KBr pellets from 4000 to 400 cm^{-1} . ^1H NMR and ^{13}C NMR spectra were recorded on a Bruker Avance (400 MHz). Fast atom bombardment mass spectra (FAB MS) were recorded on a Jeol SX 102/Da-600 mass spectrophotometer/data system using Argon/Xenon (6 kV, 10 mA) as the FAB gas. The accelerating voltage was 10 kV and spectra were recorded at room temperature. Electronic spectra

were recorded on a UV-160 A UV-Vis spectrophotometer, Shimadzu (Japan). Thermogravimetric analysis (TGA) was carried out using a 5000/2960 SDTA, TA instrument (USA) operating at a heating rate of $10^{\circ}\text{C min}^{-1}$ from 20°C to 800°C in N_2 . C, H, and N elemental analyses were performed with a model 240 Perkin Elmer elemental analyzer.

2.3. Synthesis of the ligands

2.3.1. Synthesis of 4'-(3-bromophenyl)-2,2':6',2''-terpyridine (3-bptpy). 2-Acetylpyridine (2.42 g, 20.0 mmol) was added to 70 mL ethanolic solution of 3-bromobenzaldehyde (1.85 g, 10.0 mmol). KOH pellets (1.4 g, 26 mmol) and aqueous NH_3 (30 mL, 25%, 0.425 mol) were added to the solution which was then stirred at room temperature for 8 h (scheme 1). An off-white solid formed which was collected by filtration and washed with H_2O ($3 \times 10\text{ mL}$) and ethanol ($2 \times 5\text{ mL}$). Recrystallization from CHCl_3 -MeOH gave white crystalline solid. Yield: 1.82 g, 47%, m.p.: 167 – 168°C . $^1\text{H NMR}$ (CDCl_3 , 400 MHz) δ/ppm 8.789–8.719 (m, 6 H, $\text{H}_{3,6,3',5',3'',6''}$), 8.081 (s, 1 H, $\text{H}_{\text{ph}2}$), 7.955 (dd, 2 H, $\text{H}_{4,4''}$), 7.892 (d, 1 H, $\text{H}_{\text{ph}6}$), 7.612 (d, 1 H, $\text{H}_{\text{ph}4}$), 7.436–7.397 (m, 3 H, $\text{H}_{\text{ph}5}$, $\text{H}_{5,5''}$). $^{13}\text{C NMR}$ (CDCl_3 , 100 MHz) δ/ppm 155.78 ($\text{C}_{2',6'}$), 155.7 ($\text{C}_{2,2''}$), 151.32 ($\text{C}_{\text{ph}4}$), 148.88 ($\text{C}_{6,6''}$), 140.5 ($\text{C}_{\text{ph}1}$), 137.22 ($\text{C}_{4,4''}$), 132.0 ($\text{C}_{\text{ph}2}$), 130.49 ($\text{C}_{\text{ph}5}$), 130.26 ($\text{C}_{\text{ph}4}$), 126.05 ($\text{C}_{\text{ph}6}$), 124.04 ($\text{C}_{5,5''}$), 123.14 ($\text{C}_{\text{ph}3}$), 121.54 ($\text{C}_{3,3''}$), 118.96 ($\text{C}_{3',5'}$). Anal. Calcd for $\text{C}_{21}\text{H}_{14}\text{BrN}_3$: C, 64.96; H, 3.63; N, 10.82. Found: C, 65.16; H, 3.52; N, 10.96.

2.3.2. Synthesis of 4'-(3-chlorophenyl)-2,2':6',2''-terpyridine (3-cptpy). This ligand was prepared by the method described above, but using 3-chlorobenzaldehyde (1.4 g, 10 mmol) instead of 3-bromobenzaldehyde. Yield: 1.44 g, 42%, m.p.: 152 – 153°C . $^1\text{H NMR}$ (CDCl_3 , 400 MHz) δ/ppm 8.775–8.699 (m, 6 H, $\text{H}_{3,6,3',5',3'',6''}$), 7.948–7.917 (m, 3 H, $\text{H}_{\text{ph}2}$, $\text{H}_{4,4''}$), 7.826 (d, 1 H, $\text{H}_{\text{ph}6}$), 7.471 (m, 2 H, $\text{H}_{\text{ph}4,5}$), 7.404 (dd, 2 H, $\text{H}_{5,5''}$). $^{13}\text{C NMR}$ (CDCl_3 , 100 MHz) δ/ppm 155.5 ($\text{C}_{2,2',6',2''}$), 149.14 (C_4), 140.16 ($\text{C}_{6,6''}$), 137.61 ($\text{C}_{\text{ph}1}$), 135.0 ($\text{C}_{4,4''}$), 130.27 ($\text{C}_{\text{ph}3}$), 129.16 ($\text{C}_{\text{ph}4}$), 127.42 ($\text{C}_{\text{ph}5}$), 125.68 ($\text{C}_{\text{ph}2}$),



Scheme 1. Structure of $[\text{Ru}(3\text{-bptpy})(\text{dmphen})\text{Cl}]\text{ClO}_4$.

124.13 (C_{ph6}), 121.7 (C_{5,5''}), 119.24 (C_{3,3''}), 117.36 (C_{3',5'}). Anal. Calcd for C₂₁H₁₄ClN₃: C, 73.36; H, 4.10; N, 12.22. Found: C, 73.12; H, 4.21; N, 12.36.

2.3.3. Synthesis of 4'-(2-thiophenyl)-2,2':6',2''-terpyridine (2-tptpy). This ligand was prepared by the method described above but using thiophene-2-carbaldehyde (1.12 g, 10 mmol) instead of 3-bromobenzaldehyde. Yield: 1.17 g, 37%, m.p.: 211–213°C. ¹H NMR (CDCl₃, 400 MHz) δ/ppm 8.748 (d, 2 H, H_{3,3''}), 8.714 (s, 2 H, H_{3',5'}), 8.643 (d, 2 H, H_{6,6''}), 7.873 (dd, 2 H, H_{4,4''}), 7.796 (d, 1 H, H_{Th3}), 7.448 (d, 1 H, H_{Th5}), 7.358 (dd, 2 H, H_{5,5''}), 7.172 (t, 1 H, H_{Th4}). ¹³C NMR (CDCl₃, 100 MHz) δ/ppm 155.8 (C_{2,2',6',2''}), 148.89 (C_{6,6''}), 143.48 (C_{4'}), 141.79 (C_{Th1}), 137.08 (C_{4,4''}), 128.33 (C_{Th3}), 125.97 (C_{Th2}), 123.94 (C_{5,5''}), 121.44 (C_{3,3''}), 117.28 (C_{3',5'}). Anal. Calcd for C₁₉H₁₃N₃S: C, 72.36; H, 4.15; N, 13.32. Found: C, 72.57; H, 4.03; N, 13.18.

2.3.4. Synthesis of 4'-(9-anthryl)-2,2':6',2''-terpyridine (9-atpy). This ligand was prepared by the method described above but using 9-anthraldehyde (2.06 g, 10 mmol) instead of 3-bromobenzaldehyde. Yield: 2.08 g, 51%, m.p.: 133–135°C. ¹H NMR (CDCl₃, 400 MHz) δ/ppm 8.955 (s, 1 H, H_{A10}), 8.756 (d, 2 H, H_{3,3''}), 8.495 (s, 2 H, H_{3',5'}), 8.4 (d, 2 H, H_{6,6''}), 8.053 (d, 4 H, H_{A1,A4,A5,A8}), 7.974 (dd, 2 H, H_{4,4''}), 7.573–7.503 (m, 6 H, H_{A2,A3,A6,A7}, H_{5,5''}). ¹³C NMR (CDCl₃, 100 MHz) δ/ppm 154.2 (C_{2,2',6',2''}), 148.99 (C_{6,6''}), 141.71 (C_{4'}), 137.05 (C_{4,4''}), 131.33 (C_{A9}), 128.9 (C_{A11,A12}), 128.57 (C_{A10}), 127.43 (C_{5,5''}), 126.95 (C_{A4,A5}), 126.41 (C_{A1,A8,A13,A14}), 125.4 (C_{A2,A3,A6,A7}), 125.38 (C_{3,3''}), 123.1 (C_{3',5'}). Anal. Calcd for C₂₉H₁₉N₃: C, 85.06; H, 4.68; N, 10.26. Found: C, 85.34; H, 4.81; N, 10.39.

2.4. Synthesis of the complexes

2.4.1. Synthesis of [Ru^{II}(3-bptpy)(dmphen)Cl]ClO₄ (1). [Ru^{III}(3-bptpy)Cl₃] was synthesized by a method described previously [23, 24]. [Ru^{III}(3-bptpy)Cl₃] (298 mg, 0.5 mmol), dmphen (114 mg, 0.55 mmol), excess LiCl (122 mg, 2.94 mmol), and NEt₃ (0.9 mL) were taken in 50 mL ethanol and the mixture was refluxed for 2 h under nitrogen (scheme 1). The initial dark brown color of the solution gradually changed to deep-purple. The solvent was then removed under reduced pressure. The dry mass was dissolved in a minimum volume of acetonitrile and excess saturated aqueous solution of sodium perchlorate was added. The precipitate was filtered off and washed with cold ethanol followed by ice-cold water. The product was dried in vacuum and purified using a silica column. The complex was eluted by 2 : 1 CH₂Cl₂/CH₃CN. Yield: 0.254 g, 61%, mol. wt. 832.49. IR (KBr): ν 3053 w,br; 2921 sh; 1595 m,sh; 1491 m,sh; 1089 s,sh; 753 s,sh; 627 vs,sh; 506 w,sh cm⁻¹. Anal. Calcd for C₃₅H₂₆BrCl₂N₅O₄Ru (%): C, 50.50; H, 3.15; N, 8.41. Found (%): C, 50.28; H, 3.28; N, 8.58. FAB MS: *m/z* = 833 [M]⁺, 735 [M–ClO₄ + H]⁺, 734 [M–ClO₄]⁺, 699 [M–ClO₄–Cl]⁺, 389 [3-bptpy + 2H]⁺, 311 [Ru(dmphen) + H]⁺, 209 [dmphen + H]⁺.

2.4.2. Synthesis of [Ru^{II}(3-cptpy)(dmphen)Cl]ClO₄ (2). This complex was synthesized identical to that described for [Ru^{II}(3-cptpy)(dmphen)Cl]ClO₄, with [Ru^{III}(3-cptpy)Cl₃] (276 mg, 0.5 mmol) in place of [Ru^{III}(3-bptpy)Cl₃]. Yield: 0.291 g, 74%, mol. wt. 788.04.

IR (KBr): ν 3055 w,br; 2922 sh; 1596 m,sh; 1494 m,sh; 1086 s,sh; 758 s,sh; 629 vs,sh; 511 w,sh cm^{-1} . Anal. Calcd for $\text{C}_{35}\text{H}_{26}\text{Cl}_3\text{N}_5\text{O}_4\text{Ru}$ (%): C, 53.34; H, 3.33; N, 8.89. Found (%): C, 53.12; H, 3.44; N, 9.06. FAB MS: $m/z = 789$ $[\text{M}]^+$, 691 $[\text{M}-\text{ClO}_4 + \text{H}]^+$, 653 $[\text{M}-\text{ClO}_4-\text{Cl}]^+$, 345 $[\text{3-cptpy} + 2\text{H}]^+$, 311 $[\text{Ru}(\text{dmphen}) + \text{H}]^+$, 209 $[\text{dmphen} + \text{H}]^+$.

2.4.3. Synthesis of $[\text{Ru}^{\text{II}}(\text{2-tptpy})(\text{dmphen})\text{Cl}]\text{ClO}_4$ (3). This complex was synthesized as for $[\text{Ru}^{\text{II}}(\text{3-bptpy})(\text{dmphen})\text{Cl}]\text{ClO}_4$, with $[\text{Ru}^{\text{III}}(\text{2-tptpy})\text{Cl}_3]$ (261 mg, 0.5 mmol) in place of $[\text{Ru}^{\text{III}}(\text{3-bptpy})\text{Cl}_3]$. Yield: 0.247 g, 65%, mol. wt. 759.62. IR (KBr): ν 3064 w,br; 2924 sh; 1593 m,sh; 1495 m,sh; 1085 s,sh; 764 s,sh; 626 vs,sh; 486 w,sh cm^{-1} . Anal. Calcd for $\text{C}_{33}\text{H}_{25}\text{Cl}_2\text{N}_5\text{O}_4\text{RuS}$ (%): C, 52.18; H, 3.32; N, 9.22. Found (%): C, 52.32; H, 3.47; N, 9.06. FAB MS: $m/z = 759$ $[\text{M}]^+$, 661 $[\text{M}-\text{ClO}_4 + \text{H}]^+$, 625 $[\text{M}-\text{ClO}_4-\text{Cl}]^+$, 318 $[\text{2-tptpy} + 3\text{H}]^+$, 311 $[\text{Ru}(\text{dmphen}) + \text{H}]^+$, 209 $[\text{dmphen} + \text{H}]^+$.

2.4.4. Synthesis of $[\text{Ru}^{\text{II}}(\text{9-atpy})(\text{dmphen})\text{Cl}]\text{ClO}_4$ (4). This complex was synthesized in a manner identical to that described for **1**, with $[\text{Ru}^{\text{III}}(\text{9-atpy})\text{Cl}_3]$ (308 mg, 0.5 mmol) in place of $[\text{Ru}^{\text{III}}(\text{3-bptpy})\text{Cl}_3]$. Yield: 0.294 g, 69%, mol. wt. 853.71. IR (KBr): ν 3062 w,br; 2929 sh; 1597 m,sh; 1493 m,sh; 1086 s,sh; 763 s,sh; 623 vs,sh; 492 w,sh cm^{-1} . Anal. Calcd for $\text{C}_{43}\text{H}_{31}\text{Cl}_2\text{N}_5\text{O}_4\text{Ru}$ (%): C, 60.50; H, 3.66; N, 8.20. Found (%): C, 60.27; H, 3.76; N, 8.37. FAB MS: $m/z = 853$ $[\text{M}]^+$, 755 $[\text{M}-\text{ClO}_4 + \text{H}]^+$, 719 $[\text{M}-\text{ClO}_4-\text{Cl}]^+$, 411 $[\text{9-atpy} + 2\text{H}]^+$, 311 $[\text{Ru}(\text{dmphen}) + \text{H}]^+$, 209 $[\text{dmphen} + \text{H}]^+$.

Caution: Perchlorate salts of metal complexes with organic ligands are potentially explosive. Only small amounts of material should be prepared and handled with care. The complexes described in this report have, so far, been found to be safe when used in small quantities.

2.5. DNA-binding and cleavage

Influence of DNA on MLCT band of Ru^{II} complexes was measured *via* UV-Vis absorbance spectra [25–28]. Stock solution of the complex was prepared by dissolving the complex in DMSO and diluting with buffer solution to required concentrations. The absorption titration was carried out by keeping the concentration of complex constant ($20\ \mu\text{mol L}^{-1}$) and varying the concentration of nucleic acid. Equal solution of DNA was added to both complex solution and reference solution to eliminate the absorbance of DNA itself. The change in absorbance of the MLCT band was recorded after each addition of DNA solution. The intrinsic binding constant K_b was determined according to the following equation [29]:

$$[\text{DNA}]/(\varepsilon_a - \varepsilon_f) = [\text{DNA}]/(\varepsilon_b - \varepsilon_f) + 1/K_b(\varepsilon_b - \varepsilon_f),$$

where $[\text{DNA}]$ is the concentration of DNA in base pairs, the apparent absorption coefficient ε_a , ε_f , and ε_b correspond to $A_{\text{obs}}/[\text{Ru}]$, the extinction coefficient for the free ruthenium complex for each addition of DNA, and the extinction coefficient for the ruthenium complex in the fully bound form, respectively. In plots of $[\text{DNA}]/(\varepsilon_a - \varepsilon_f)$ *versus* $[\text{DNA}]$, K_b is given by the ratio of slope to the y -intercept.

Effect of EB or Ru^{II} complexes on relative viscosity of DNA solution was measured using a Cannon-Ubbelohde viscometer (3 mL capacity) maintained at $27.0 (\pm 0.1)^\circ\text{C}$ in

a thermostatic jacket. DNA concentration was chosen to make changes in the slope maximally distinguishable. A 3.0 mmol L^{-1} stock solution of each Ru^{II} complex was prepared. A $400 \mu\text{mol L}^{-1}$ solution of Herring Sperm DNA was titrated with the Ru^{II} complex. The Ru^{II} complex to DNA concentration ratio was maintained in the range 0–0.2. Flow time was measured with a digital stopwatch. The flow time of each sample was measured three times and an average flow time calculated. Data were represented graphically as $(\eta/\eta_0)^{1/3}$ versus concentration ratio ($[\text{Complex}]/[\text{DNA}]$) [30], where η is viscosity of DNA solution in the presence of complex and η_0 is viscosity of DNA solution alone. Viscosity values were calculated from the observed flow time of DNA-containing solutions ($t > 100 \text{ s}$) corrected for the flow time of buffer alone (t_0), $\eta = t - t_0$.

Gel electrophoresis of pUC19 DNA was carried out in TAE buffer (0.04 mol L^{-1} Tris-Acetate, pH 8, 0.001 mol L^{-1} EDTA). Supercoiled (SC) pUC19 DNA ($100 \mu\text{g mL}^{-1}$) was treated with $100 \mu\text{mol L}^{-1}$ samples of the metal complexes and the mixtures were incubated at 37°C for 240 min. All reactions were quenched by addition of $3 \mu\text{L}$ gel loading dye (0.25% bromophenol blue, 40% sucrose, 0.25% xylene cyanol FF, and 200 mmol L^{-1} EDTA). The aliquots were loaded directly onto 1% agarose gel and electrophoresed at 50 V in 1X TAE buffer for 3 h. Gel was stained with $0.5 \mu\text{g mL}^{-1}$ of EB, and visualized by UV light and photographed for analysis. After electrophoresis, the extent of cleavage was measured from the intensities of the bands using the AlphaDigiDocTM RT. Version V.4.0.0 PC-Image software.

3. Results and discussion

3.1. Thermogravimetric and electronic absorption analysis

Absence of coordinated and crystalline water molecules were confirmed from TGA. The TG curve shows no weight loss from 80°C to 180°C . The electronic spectra of the ligands and Ru^{II} complexes were recorded in DMSO and relevant data are summarized in table 1. The electronic spectra of ligands show only one band at $\sim 285 \text{ nm}$. The electronic spectra of complexes consist of three well-defined bands at 250–500 nm. Similar bands are observed for $[\text{Ru}(\text{dpphen})(\text{terpy})\text{Cl}]\text{PF}_6$ reported by Yoshikawa *et al.* [31]. The UV-Vis spectrum of the complexes exhibits the typical MLCT band between 488 and 492 nm. The two higher energy absorption bands were observed from 274 to 281 nm and 309 to 311.5 nm, attributed to ligand-centered transitions $\text{dmphen}(\pi) \rightarrow \text{dmphen}(\pi^*)$ and $\text{terpy}(\pi) \rightarrow \text{terpy}(\pi^*)$, respectively [30].

3.2. Infrared spectroscopy

Aromatic C–H stretching band appeared at 3060 cm^{-1} . A sharp band at 2925 cm^{-1} is due to $\nu_{\text{C-H}}$ of methyl. Sharp bands with medium intensity at 1600 and 1495 cm^{-1} are characteristics of aromatic ring stretching. An intense, sharp band at $\sim 760 \text{ cm}^{-1}$ is characteristic of ring deformations and C–H out-of-plane deformations. The presence of perchlorate is confirmed by the very strong, broad band at $\sim 1085 \text{ cm}^{-1}$ and the strong, sharp band at 625 cm^{-1} [32]. A weak, sharp band at $486\text{--}511 \text{ cm}^{-1}$ is characteristic of Ru–N stretch. A Ru–Cl stretch would be expected less than 400 cm^{-1} [33].

Table 1. Electronic spectral data for the ruthenium(II) complexes.

Complex	λ_{\max} (nm) ($\epsilon/\text{dm}^3 \text{ mol}^{-1} \text{ cm}^{-1}$)	
	$\pi \rightarrow \pi^*$	MLCT
1	276.5 (60,100), 311.5 (43,600)	489.5 (19,950)
2	274.0 (64,600), 309.5 (46,300)	488.0 (21,100)
3	281.5 (45,400), 310.0 (43,100)	491.5 (18,400)
4	275.0 (39,300), 309.0 (43,000)	494.0 (16,700)

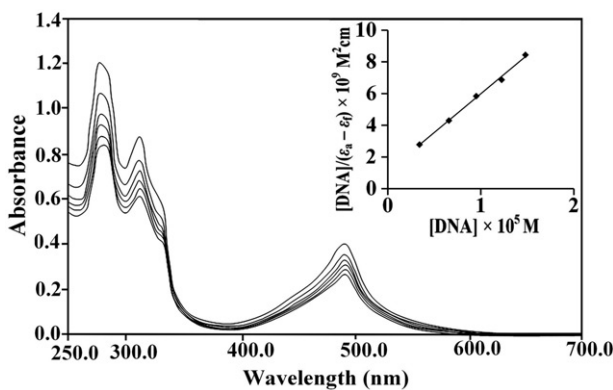


Figure 1. Electronic absorption spectra of $[\text{Ru}^{\text{II}}(3\text{-btpy})(\text{dmphen})\text{Cl}]\text{ClO}_4$ with increasing amounts of Herring Sperm DNA in phosphate buffer ($\text{Na}_2\text{HPO}_4/\text{NaH}_2\text{PO}_4$, pH 7.2). $[\text{complex}] = 20 \mu\text{mol L}^{-1}$, $[\text{DNA}] = 0\text{--}18.4 \mu\text{mol L}^{-1}$ with incubation period of 15 min at 37°C . Inset: plots of $[\text{DNA}]/(\epsilon_a - \epsilon_f)$ vs. $[\text{DNA}]$ for the titration of DNA with Ru^{II} complexes.

3.3. Absorption titration

Complexes binding to DNA through intercalation/partial intercalation usually result in hypochromism and bathochromism [34]. When the complex intercalates with base pairs of DNA, the π^* orbital of the intercalated ligand of the complex couples with π orbital of the base pairs, thus decreasing the $\pi\text{--}\pi^*$ transition energy [35]. Electrostatic interaction of complex with DNA shows lower hypochromicity with no bathochromic shift [36]. Absorption titration of the complexes was performed using Herring Sperm DNA. As the concentration of DNA increases, the intensity of the MLCT band decreases along with a red shift (figure 1). The extent of the hypochromism commonly parallels the intercalative binding strength.

All complexes show decrease in the MLCT transition from 8.9% to 15.4% along with red shift of 2 and 3 nm (table 2). The highest hypochromism was observed for **1**, indicating **1** interacts with DNA more strongly. These results suggest that the complexes bind to DNA *via* classical intercalation or partial intercalation. More confirmation regarding to the binding mode of the complexes will be obtained from viscosity measurement.

Quantitative determination of DNA-binding affinity of the complexes can be done by finding the intrinsic binding constants (K_b). From decay of MLCT band absorbance, the K_b values for **1–4** are $0.893\text{--}4.45 \times 10^4 (\text{mol L}^{-1})^{-1}$, comparable to those observed

Table 2. Electronic absorption data upon addition of Herring Sperm DNA.

Complex	λ_{\max} (nm)			Hypochromism H^a (%)	Binding constant K_b ((mol L ⁻¹) ⁻¹)
	Free	Bound	$\Delta\lambda$		
1	489.5	492.5	3	15.4	4.45×10^4
2	488.0	490.0	2	14.6	3.86×10^4
3	491.5	494.5	3	13.9	2.84×10^4
4	494.0	496.0	2	8.9	8.93×10^3

$$^a H\% = 100 \times (A_{\text{free}} - A_{\text{bound}}) / A_{\text{free}}$$

for [Ru(k³-tpy)(PPh₃)₂Cl]BF₄ · 0.5H₂O · 0.5CH₂Cl₂ (4.1×10^4 (mol L⁻¹)⁻¹), [Ru(k³-tpy)(AsPh₃)₂Cl]BF₄ · H₂O (4.5×10^4 M⁻¹) [37], [Ru(tpy)(ptmi)](ClO₄)₂ (1.35×10^4 (mol L⁻¹)⁻¹), [Ru(tpy)(pti)](ClO₄)₂ (3.03×10^4 (mol L⁻¹)⁻¹), [Ru(tpy)(ptni)](ClO₄)₂ (5.63×10^4 (mol L⁻¹)⁻¹) [38], [Ru(tpy)(PHBI)](ClO₄)₂ · H₂O (3.2×10^4 (mol L⁻¹)⁻¹) and higher than [Ru(tpy)(PHNI)](ClO₄)₂ · 2H₂O (1.6×10^3 (mol L⁻¹)⁻¹) [39]. The reason for the lower K_b value is the non-planarity of terpyridines and methyl substitution on phenanthroline. Substitution on the 2- and 9-positions of phenanthroline may cause steric constraints near the Ru^{II} core when the complex intercalates into DNA base pairs. The methyls may come into proximity of base pairs at the intercalation sites. Absence of planarity of the phenyl, thiophene, and anthracene moiety with the basic terpyridine unit decreases the binding strength of complexes [40].

3.4. Viscosity measurement

Viscosity measurements were carried out to further clarify interaction of the metal complexes with DNA. Relative viscosity of the DNA solution increases in classical intercalation because the base pairs are separated to accommodate the binding ligand resulting in lengthening of the DNA. Partial and/or non-classical intercalation decreases relative viscosity of DNA, because it may bend DNA helix decreasing effective length of DNA [41]. Electrostatic interaction of compound with DNA does not affect relative viscosity of DNA [42]. The effect of increasing amount of EB and complexes on the relative viscosity of DNA is shown in figure 2. For all complexes, relative viscosity of DNA solution decreases upon increasing the concentration ratio of complex to DNA. Considering the results of absorption titration and viscosity measurements, it can be concluded that the complexes partially intercalate to DNA, similar to previously reported results by Rao *et al.*, Chaveerach *et al.*, and Sun *et al.* for the partial intercalation mode of binding [43–45].

3.5. DNA cleavage activity

Plasmid cleavage activity of the complexes was studied on pUC19 by loading the plasmid onto agarose gel followed by electrophoresis. Upon electrophoresis of plasmid DNA, fastest migration is observed for SC form, whereas the slowest moving is open circular (OC) form, generated when one strand is nicked. Linear (L) form, generated when both the strands are cleaved, migrates between SC and OC. Figure 3 shows the electrophoretic separation of pUC19 DNA reacted upon complexes under aerobic

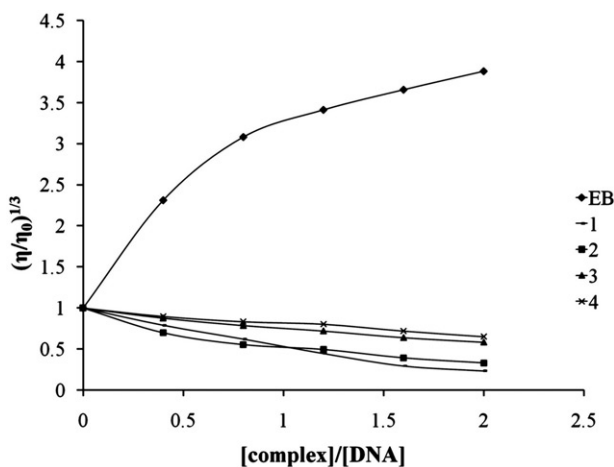


Figure 2. Effect on relative viscosity of DNA under the influence of increasing amounts of ethidium bromide and complexes at $27 \pm 0.1^\circ\text{C}$ in phosphate buffer ($\text{Na}_2\text{HPO}_4/\text{NaH}_2\text{PO}_4$, pH 7.2).

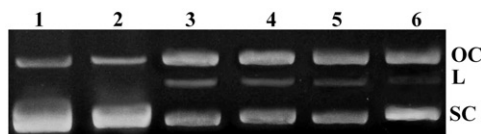


Figure 3. Agarose gel (1%) of pUC19 ($100 \mu\text{g mL}^{-1}$) at 37°C in TE buffer (pH 8) with $100 \mu\text{mol L}^{-1}$ compounds incubated for 240 min. Lane 1, DNA control; lane 2, RuCl_3 ; lane 3, $[\text{Ru}^{\text{II}}(3\text{-bptpy})(\text{dmphen})\text{Cl}]\text{ClO}_4$; lane 4, $[\text{Ru}^{\text{II}}(3\text{-cptpy})(\text{dmphen})\text{Cl}]\text{ClO}_4$; lane 5, $[\text{Ru}^{\text{II}}(2\text{-tptpy})(\text{dmphen})\text{Cl}]\text{ClO}_4$; lane 6, $[\text{Ru}^{\text{II}}(9\text{-atpy})(\text{dmphen})\text{Cl}]\text{ClO}_4$.

condition. The data of the percentage cleavage of DNA, presented in figure 4, reveal that the complexes can cleave DNA more efficiently than the metal salt. Complex **1** shows the highest percentage conversion of SC form into OC and L forms (47%), while **4** shows lowest conversion of SC form (27%). This suggests hydrolytic cleavage of DNA by the complexes, similar to previously reported ruthenium(II) complexes [46, 47].

4. Conclusion

Quantitative binding strengths of complexes were measured by calculating intrinsic binding constants. The K_b values obtained are $(0.893\text{--}4.45) \times 10^4 (\text{mol L}^{-1})^{-1}$. The data show that the binding strength of **1** is greater than other complexes. Planarity and steric effects of the ligands affect the binding affinity of the complex. Presence of electron withdrawing group enhances binding ability of the complex. Decrease in relative viscosity of the DNA solution reveals that the complexes bind DNA *via* partial intercalation, similar to partial intercalators synthesized by various research groups.

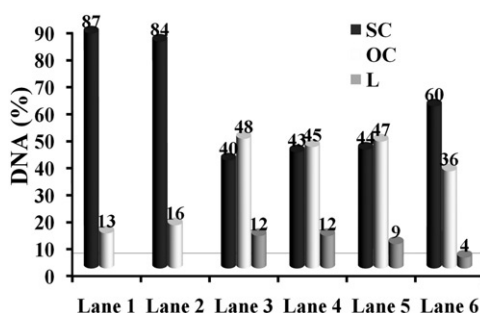


Figure 4. The percentage of SC, OC, and L forms of pUC19 DNA produced by $100\ \mu\text{mol L}^{-1}$ of $[\text{Ru}^{\text{II}}(3\text{-bptpy})(\text{dmphen})\text{Cl}]\text{ClO}_4$, $[\text{Ru}^{\text{II}}(3\text{-cptpy})(\text{dmphen})\text{Cl}]\text{ClO}_4$, $[\text{Ru}^{\text{II}}(2\text{-tptpy})(\text{dmphen})\text{Cl}]\text{ClO}_4$, and $[\text{Ru}^{\text{II}}(9\text{-atpy})(\text{dmphen})\text{Cl}]\text{ClO}_4$ complexes at 240 min.

DNA damage data reveal that the cleavage efficiency of the complexes is more than metal salt. Ruthenium(II) complexes cleave DNA hydrolytically.

Acknowledgments

The authors thank Head, Department of Chemistry, and Dr Thakkar, BRD School of Bioscience, Sardar Patel University, India for making it convenient to work in laboratory, and U.G.C. for providing financial assistance of UGC grant 40–95/2011(SR).

References

- [1] W.J. Mei, X.Y. Wei. *Trans. Met. Chem.*, **32**, 685 (2007).
- [2] Y.J. Liu, X.Y. Guan, X.Y. Wei, L.X. He, W.J. Mei, J.H. Yao. *Trans. Met. Chem.*, **33**, 289 (2008).
- [3] D.L. Arockiasamy, S. Radhika, R. Parthasarathi, B.U. Nair. *Eur. J. Med. Chem.*, **44**, 2044 (2009).
- [4] S.C. Morgan, F.H. Burstall. *J. Chem. Soc.*, **20** (1931).
- [5] M. Grätzel. *Inorg. Chem.*, **44**, 6841 (2005).
- [6] E. Baranoff, J.P. Collin, L. Flamigni, J.P. Sauvage. *Chem. Soc. Rev.*, **33**, 147 (2004).
- [7] P.W. Du, J. Schneider, P. Jarosz, R. Eisenberg. *J. Am. Chem. Soc.*, **128**, 7726 (2006).
- [8] B. Song, G. Wang, M. Tan, J. Yuan. *J. Am. Chem. Soc.*, **128**, 13442 (2006).
- [9] R. Shunmugam, G.N. Tew. *J. Am. Chem. Soc.*, **127**, 13567 (2005).
- [10] K. Ketomaki, H. Lonnberg. *Bioconjugate Chem.*, **17**, 1063 (2006).
- [11] L.A. Levine, C.M. Morgan, K. Ohr, M.E. Williams. *J. Am. Chem. Soc.*, **127**, 16764 (2005).
- [12] A. Fussl, A. Schleifenbaum, M. Goritz, A. Riddell, C. Schultz, R. Kramer. *J. Am. Chem. Soc.*, **128**, 5986 (2006).
- [13] K. Karidi, A. Garoufis, A. Tsipis, N. Hadjiliadis, H. den Dulck, J. Reedijk. *Dalton Trans.*, 1176 (2005).
- [14] R.N. Patel, N. Singh, K.K. Shukla, V.L.N. Gundla, U.K. Chauhan. *Spectrochim. Acta, Part A*, **63**, 21 (2006).
- [15] M. Benmelouka, J. Van Tol, A. Borel, M. Port, L. Helm, L.C. Brunel, A.E. Merbach. *J. Am. Chem. Soc.*, **128**, 7807 (2006).
- [16] K. Kanaizuka, S. Kato, H. Moriyama, C. Pac. *Chem. Lett.*, **35**, 1036 (2006).
- [17] K.Y.K. Man, H.L. Wong, W.K. Chan, A.B. Djurišić, E. Beach, S. Rozveld. *Langmuir*, **22**, 3368 (2006).
- [18] C. Bhaumik, S. Das, D. Saha, S. Dutta, S. Baitalik. *Inorg. Chem.*, **49**, 5049 (2010).
- [19] G. Sathyaraj, T. Weyhermuller, B. Unni Nair. *J. Chem. Crystallogr.*, **41**, 353 (2011).
- [20] A. Jain, J. Wang, E.R. Mashack, B.S.J. Winkel, K.J. Brewer. *Inorg. Chem.*, **48**, 9077 (2009).

- [21] G. Sathyaraj, T. Weyhermuller, B. Unni Nair. *Eur. J. Med. Chem.*, **45**, 284 (2010).
- [22] M.N. Patel, P.B. Pansuriya. *Appl. Organomet. Chem.*, **21**, 739 (2007).
- [23] N. Yoshikawa, S. Yamabe, N. Kanehisa, Y. Kai, H. Takashima, K. Tsukahara. *Inorg. Chim. Acta*, **359**, 4585 (2006).
- [24] N. Chanda, S.M. Mobin, V.G. Puranik, A. Datta, M. Niemeyer, G. Lahiri. *Inorg. Chem.*, **43**, 1056 (2004).
- [25] H. Deng, J. Li, K.C. Zheng, Y. Yang, H. Chao, L.N. Ji. *Inorg. Chim. Acta*, **358**, 3430 (2005).
- [26] Mudasir, N. Yoshioka, H. Inoue. *J. Inorg. Biochem.*, **77**, 239 (1999).
- [27] L. Fin, P. Yang. *J. Inorg. Biochem.*, **68**, 79 (1997).
- [28] Q.L. Zhang, J.G. Liu, H. Chao, G.Q. Xue, L.N. Ji. *J. Inorg. Biochem.*, **83**, 49 (2001).
- [29] H. Chao, W.J. Mei, Q.W. Huang, L.N. Ji. *J. Inorg. Biochem.*, **92**, 165 (2002).
- [30] Y.B. Zeng, N. Yang, W.S. Liu, N. Tang. *J. Inorg. Biochem.*, **97**, 258 (2003).
- [31] N. Yoshikawa, S. Yamabe, N. Kanehisa, Y. Kai, H. Takashima, K. Tsukahara. *Inorg. Chim. Acta*, **359**, 4585 (2006).
- [32] C. Eva, A.G.C. Hotze, D.M. Tooke, A.L. Spek, J. Reedijk. *Inorg. Chim. Acta*, **359**, 830 (2006).
- [33] S. Goswami, A.R. Chakravarty, A. Chakravorty. *Inorg. Chem.*, **21**, 2737 (1982).
- [34] J.R.J. Sorenson. *J. Med. Chem.*, **27**, 1747 (1982).
- [35] R. Indumathy, S. Radhika, M. Kanthimathi, T. Weyhermuller, B.U. Nair. *J. Inorg. Biochem.*, **101**, 434 (2007).
- [36] M.F. Iskander, L. El-Sayed, N.M.H. Salem, R. Warner, W. Haase. *J. Coord. Chem.*, **58**, 125 (2005).
- [37] S. Sharma, S.K. Singh, M. Chandra, D.S. Pandey. *J. Inorg. Biochem.*, **99**, 458 (2005).
- [38] Y.J. Liu, J.C. Chen, F.H. Wu, K.C. Zheng. *Trans. Met. Chem.*, **34**, 297 (2009).
- [39] C.W. Jiang, H. Chao, H. Li, L.N. Ji. *J. Inorg. Biochem.*, **93**, 247 (2003).
- [40] R. Indumathy, M. Kanthimathi, T. Weyhermuller, B.U. Nair. *Polyhedron*, **27**, 3443 (2008).
- [41] N. Wang, Q.Y. Lin, J. Feng, Y.L. Zhao, Y.J. Wang, S.K. Li. *Inorg. Chim. Acta*, **363**, 3399 (2010).
- [42] M. Chauhan, F. Arjmand. *J. Organomet. Chem.*, **692**, 5156 (2007).
- [43] U. Chaveerach, A. Meenongwa, Y. Trongpanich, C. Soikum, P. Chaveerach. *Polyhedron*, **29**, 731 (2010).
- [44] S. Satyanarayana, J.C. Cabrowiak, J.B. Chaires. *Biochemistry*, **32**, 2573 (1993).
- [45] J. Sun, S. Wu, Y. An, J. Liu, F. Gao, L.N. Ji, Z.W. Mao. *Polyhedron*, **27**, 2845 (2008).
- [46] M.S. Deshpande, A.A. Kumbhar, A.S. Kumbhar. *Inorg. Chem.*, **46**, 5450 (2007).
- [47] S.R. Grguric-Sipkaa, R.A. Vilaplana, J.M. Perez, M.A. Fuertesc, C. Alonsoc, Y. Alvarez, T.J. Sabo, F. Gonzalez-Vlchez. *J. Inorg. Biochem.*, **97**, 215 (2003).